

DIRECT CONSTRAINTS ON THE DARK MATTER SELF-INTERACTION CROSS-SECTION FROM THE MERGING GALAXY CLUSTER 1E 0657–56

M. MARKEVITCH¹, A. H. GONZALEZ², D. CLOWE^{3,4}, A. VIKHLININ^{1,5}, W. FORMAN¹, C. JONES¹, S. MURRAY¹, W. TUCKER^{1,6}
ApJ in press; astro-ph/0309303 v2

ABSTRACT

We compare new maps of the hot gas, dark matter, and galaxies for 1E 0657–56, a cluster with a rare, high-velocity merger occurring nearly in the plane of the sky. The X-ray observations reveal a bullet-like gas subcluster just exiting the collision site. A prominent bow shock gives an estimate of the subcluster velocity, 4500 km s⁻¹, which lies mostly in the plane of the sky. The optical image shows that the gas lags behind the subcluster galaxies. The weak-lensing mass map reveals a dark matter clump lying ahead of the collisional gas bullet, but coincident with the effectively collisionless galaxies. From these observations, one can directly estimate the cross-section of the dark matter self-interaction. That the dark matter is not fluid-like is seen directly in the X-ray – lensing mass overlay; more quantitative limits can be derived from three simple independent arguments. The most sensitive constraint, $\sigma/m < 1 \text{ cm}^2 \text{ g}^{-1}$, comes from the consistency of the subcluster mass-to-light ratio with the main cluster (and universal) value, which rules out a significant mass loss due to dark matter particle collisions. This limit excludes most of the 0.5–5 cm² g⁻¹ interval proposed to explain the flat mass profiles in galaxies. Our result is only an order-of-magnitude estimate which involves a number of simplifying, but always conservative, assumptions; stronger constraints may be derived using hydrodynamic simulations of this cluster.

Subject headings: dark matter — galaxies: clusters: individual (1E0657–56) — galaxies: formation — large scale structure of universe

1. INTRODUCTION

1E 0657–56, one of the hottest and most X-ray luminous galaxy clusters known, was discovered by Tucker et al. (1995). It was first observed by *Chandra* in October 2000 for 24 ks. That observation revealed a bullet-like, relatively cool subcluster just exiting the core of the main cluster, with a prominent bow shock (Markevitch et al. 2002, hereafter M02). A comparison of the X-ray and optical images revealed a galaxy subcluster just ahead of the gas “bullet”, which led M02 to suggest that this unique system could be used to determine whether dark matter is collisional or collisionless, if only one could map the mass distribution in the subcluster. Apart from the obvious interest for the still unknown nature of dark matter, the possibility of it having a nonzero self-interaction cross-section has far-reaching astrophysical implications (Spergel & Steinhardt 2000; for more discussion see §3.2 below).

Just such a map of the dark matter distribution in 1E 0657–56 has recently been obtained by Clowe, Gonzalez, & Markevitch (2004, hereafter C04) from weak lensing data. It reveals a dark matter clump coincident with the centroid of the galaxies (Fig. 1a). C04 also derived M/L ratios of the main cluster and the subcluster and found them in agreement with each other and with other clusters’ values. In addition, *Chandra* re-observed 1E 0657–56 for 70 ks in July 2002, from which a more accurate estimate of the shock Mach number was derived using the gas density jump at the shock, $M = 3.2^{+0.8}_{-0.6}$ (all uncertainties 68%), which corresponds to a

shock (and bullet subcluster) velocity of $v_s = 4500^{+1100}_{-800} \text{ km s}^{-1}$ (Markevitch et al., in prep., hereafter M04). The new X-ray data also further clarified the geometry of the merger.

In this paper, we combine these new optical and X-ray data to constrain the self-interaction cross-section of dark matter particles. We use $\Omega_0 = 0.3$, $\Omega_\Lambda = 0.7$, $H_0 = 70 \text{ km s}^{-1} \text{ Mpc}^{-1}$, for which $1'' = 4.42 \text{ kpc}$ at the cluster redshift $z = 0.296$.

2. COLLISIONAL CROSS-SECTION ESTIMATES

The dark matter collisional cross-section, σ , can be constrained from the 1E 0657–56 data by at least three independent methods, using simple calculations described in the sections below. They are based on the observed gas–dark matter offset, the high subcluster velocity, and the subcluster survival. First, we give the main assumptions that will go into these calculations.

There are two estimates of the total masses of the subcluster and the main cluster — from the galaxy velocity dispersion (Barrera et al. 2002) and from weak lensing (C04). Given the disturbed state of this system, virial or hydrostatic mass estimates (either from galaxy velocities or the gas temperature) can be incorrect, and we chose to use the direct weak lensing measurements from C04 even though their formal statistical accuracy is poorer. The main cluster’s lensing signal can be fit by a King mass profile $\rho = \rho_0(1 + r^2/r_c^2)^{-3/2}$ with best-fit parameters $\rho_0 \simeq 2.6 \times 10^{-25} \text{ g cm}^{-3}$ and $r_c \simeq 210 \text{ kpc}$ (C04). These two parameters are degenerate so their individual error bars are not meaningful; the quantity of interest to us is the central mass column density (approximately proportional to $\rho_0 r_c$), which is measured with a 16% accuracy. This mass profile is very close to the Barrera et al. NFW profile at all radii outside the core. A King profile is marginally preferred over an NFW profile (also acceptable statistically).

The projected mass excess created by the subcluster is detected in the lensing data with a 3.0σ significance. The subcluster mass signal is detected to $r \simeq 150\text{--}200 \text{ kpc}$ from the

¹ Harvard-Smithsonian Center for Astrophysics, 60 Garden St., Cambridge, MA 02138; maxim@head.cfa.harvard.edu

² Department of Astronomy, University of Florida

³ Institut für Astrophysik und Extraterrestrische Forschung der Universität Bonn, Germany

⁴ Stewart Observatory, University of Arizona

⁵ IKI, Moscow, Russia

⁶ University of California at San Diego

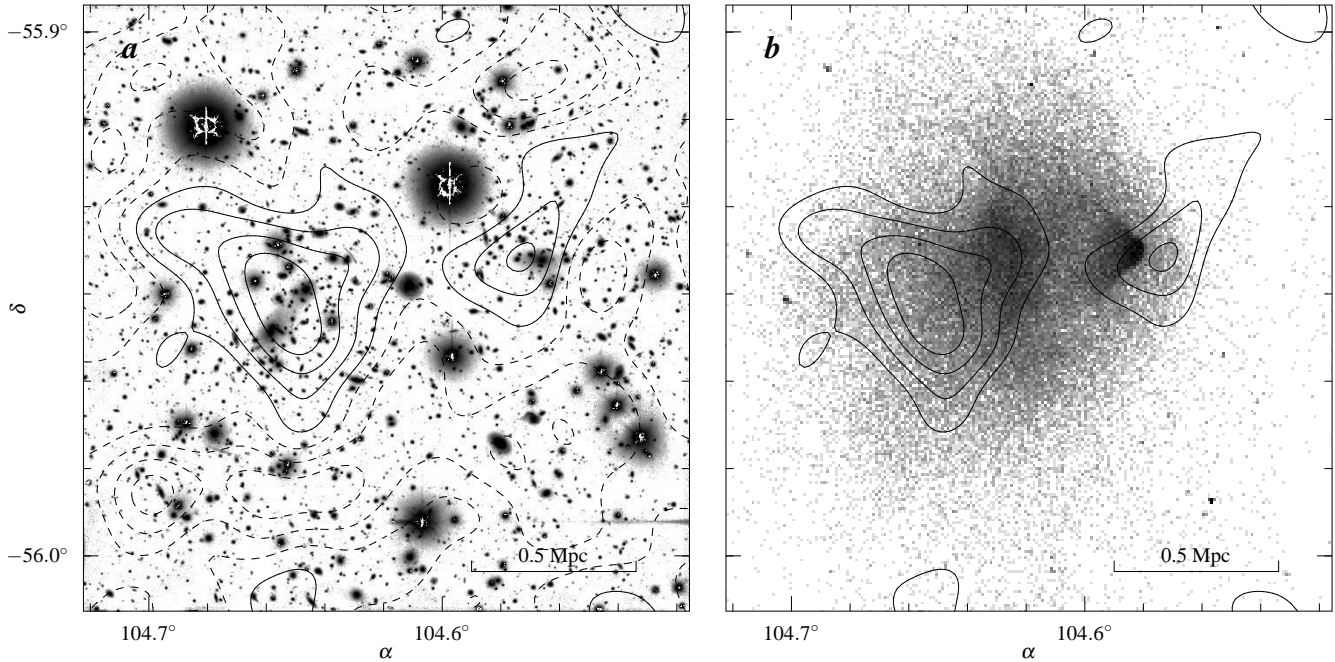


FIG. 1.— (a) Overlay of the weak lensing mass contours on the optical image of 1E0657–56. Dashed contours are negative (relative to an arbitrary zero level). The subcluster’s DM peak is coincident within uncertainties with the centroid of the galaxy concentration. (b) Overlay of the mass contours on the X-ray image (only the upper 4 of those in panel *a* are shown for clarity). The gas bullet lags behind the DM subcluster.

mass (or galaxy) peak, beyond which the subcluster may be tidally stripped (C04). The lensing-derived subcluster mass ($M \simeq 7 \times 10^{13} M_{\odot}$) is significantly higher than the Barrena et al. estimate, but the latter result was based on only 7 galaxies and the equilibrium assumption, thus could easily be biased. The current lensing data accuracy is not sufficient to derive an exact mass distribution for the subcluster, but our estimates below are not particularly sensitive to it, being mostly determined by its overall projected mass. For the sake of modeling, we will adopt a King profile with $r_c = 70$ kpc and $\rho_0 = 1.3 \times 10^{-24} \text{ g cm}^{-3}$, truncated at $r_{\text{tr}} = 150$ kpc, which adequately describes the lensing data.

The subcluster is assumed to have passed (once) close to the center of the main cluster. This is supported by the X-ray image (Fig. 1*b*), the gas temperature map (M04) and their comparison with the radio halo map (Govoni et al. 2004; Liang et al. 2000). A cooler North-South bar in the X-ray image between the two dark matter clumps appears to be an edge-on pancake-like remnant of the merged main cluster’s gas core and the subcluster’s outer atmosphere (stripped from what is now the gas bullet), suggesting that the subcluster has passed straight through the densest cluster region (M04). The line-of-sight velocity of the subcluster relative to the main cluster is about 600 km s^{-1} (Barrena et al. 2002); combined with the X-ray-measured Mach number, it gives an angle of only $\sim 8^\circ$ between the direction of motion and the plane of the sky. The sharpness of the shock front also confirms that the subcluster is presently moving very nearly in the plane of the sky (M02). From all the above, it is reasonable to assume that the subcluster has passed through the core of the main cluster.

The accuracy of our qualitative cross-section estimates will be determined by the validity of this and other assumptions (given below where relevant) to a greater degree than by the measurement uncertainties, so below we will omit the mea-

surement error propagation for clarity.

2.1. The gas — dark matter offset

The most remarkable feature in Fig. 1*b* is a $\sim 23''$ offset between the subcluster’s DM centroid and the gas bullet, which is at least 2σ -significant (C04). C04 use this fact as a direct proof of dark matter existence, as opposed to modified gravity hypotheses (Milgrom 1983 and later works) in which one would expect the lensing mass peak to be associated with the gas — the dominant visible mass component. For our purposes, this offset means that the scattering depth of the dark matter subcluster w.r.t. collisions with the flow of dark matter particles cannot be much greater than 1. Otherwise the DM subcluster would behave as a clump of fluid, experiencing stripping and drag deceleration, similar to that of the gas bullet (assuming the same gas mass fraction in the main cluster and the subcluster), and there would be no offset between the gas and dark matter. The subcluster’s scattering depth is

$$\tau_s = \frac{\sigma}{m} \Sigma_s, \quad (1)$$

where σ is the DM collision cross-section, m is its particle mass, and Σ_s is the DM mass surface density of the subcluster. The surface density averaged over the face of the subcluster within $r = r_{\text{tr}}$ is $\Sigma_s \simeq 0.2 \text{ g cm}^{-2}$. Assuming spherical symmetry and requiring that $\tau_s < 1$, we obtain

$$\frac{\sigma}{m} < 5 \text{ cm}^2 \text{ g}^{-1}. \quad (2)$$

The surface density toward the subcluster center is several times higher, so by using an average we obtain a conservative upper limit.

Another remarkable feature in Fig. 1*a* is the coincidence of the subcluster’s DM and galaxy centroids within their uncertainties (C04). To avoid an easily made mistake, we should

note here that the subcluster galaxies, although effectively collisionless, do not give us the position at which the subcluster would be in the absence of the DM collisions. The galaxies are gravitationally bound to the DM clump and will be dragged back by it, should it experience any deceleration from the DM collisions. This can be taken into account, and a limit on the offset between the DM and galaxy centroids can indeed be used to derive an independent σ/m constraint; however, it requires more accurate centroid positions than currently available.

2.2. The high velocity of the subcluster

The observed velocity of the subcluster, $v_s = 4500 \text{ km s}^{-1}$, is in good agreement with the expected free-fall velocity onto the main cluster. For our main cluster's mass profile, a small subcluster falling from a large distance should acquire 4400 km s^{-1} at core passage, decelerating to 3500 km s^{-1} at the current 0.66 Mpc off-center distance of the subcluster. Since the cluster peculiar velocities are small, such an agreement strongly suggests that the subcluster could not have lost much of its momentum to drag forces. Drag is created by putative DM particle collisions, as well as the gravitational pull of the gas being stripped from the subcluster and of the tidally-stripped outer subcluster mass, and by dynamical friction as the moving subcluster disturbs the main cluster's matter distribution. We will conservatively disregard the latter three (all of which are relatively small effects) and assume, for a qualitative estimate, that the loss of velocity due to the DM collisions, compared to free fall, is less than 1000 km s^{-1} , accumulated along the way through the main cluster.

We will now derive the drag force on the subcluster from the DM particle collisions. The subcluster will be decelerated by collisions when its particles acquire a momentum component opposite to the subcluster's velocity and then transfer all or part of it to the whole subcluster via gravitational interactions. We assume for simplicity that (a) dark matter particles have no peculiar velocities, and (b) the subcluster's gravity is felt by the particles, and vice versa, as long as the particle is within a fiducial radius $r' = 2r_{\text{tr}}$ of the subcluster (the result will not depend qualitatively on r' in the range $r_{\text{tr}} - \infty$). We further assume that a particle transfers all of its momentum to the subcluster if its post-collision velocity is insufficient to escape beyond r' . Faster-scattered particles retard the cluster only until they reach r' . The critical velocity that a subcluster particle needs to reach r' , mass-averaged (in the *rms* sense) over the subcluster mass profile, is $V \simeq 1900 \text{ km s}^{-1}$. Use of this average value lets us make a further simplifying assumption that all collisions occur at the subcluster center. We also conservatively disregard multiple scattering in the subcluster; the adequacy of this assumption will be addressed below.

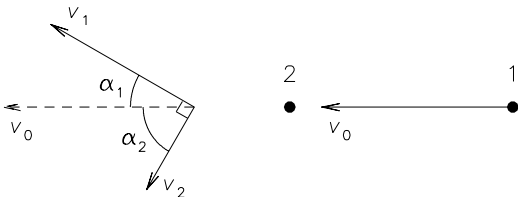


FIG. 2.— Collision of two equal-mass particles in the subcluster reference frame.

An elastic collision of two equal-mass particles proceeds as shown in Fig. 2. In the subcluster's reference frame, particle 2 is at rest and particle 1, in the incoming flow, collides with it with a velocity

$$v_0 = \sqrt{v_s^2 + V^2} \approx 4800 \text{ km s}^{-1}, \quad (3)$$

where v_s is the subcluster's velocity and the relatively small increase is because of the subcluster's gravitational pull within $r = r'$. Particle 1 scatters at an angle $\alpha_1 > 0$ with a velocity v_1 , while particle 2 acquires a velocity v_2 at an angle $\alpha_2 > 0$. From energy and momentum conservation, $\alpha_1 + \alpha_2 = \pi/2$ and the velocities are

$$v_1 = v_0 \cos \alpha_1, \quad v_2 = v_0 \sin \alpha_1. \quad (4)$$

As a result of each collision, the subcluster acquires a net momentum along the v_0 direction, $p = p_0 + p_1 + p_2$, where

$$p_0 = m(v_s - v_0) \quad (5)$$

comes from the infalling particle (which carries back exactly $-p_0$ if it passes through the subcluster without scattering), and p_i ($i = 1, 2$) comes from the respective outbound particle. If $v_i < V$ then

$$p_i = m v_i \cos \alpha_i \quad (6)$$

(the particle transfers all its momentum to the subcluster), while for $v_i > V$,

$$p_i = m \left[v_i - (v_i^2 - V^2)^{1/2} \right] \cos \alpha_i. \quad (7)$$

For our particular mass and velocity, at least one particle always escapes beyond r' . If both escape, which occurs in collisions with $\alpha_e < \alpha_1 < \frac{\pi}{2} - \alpha_e$ ($\alpha_e \simeq 23^\circ$ for our parameters), the momentum loss by the subcluster as a function of the scattering angle α_1 is (combining eqs. 5, 7, 3, and 4):

$$p_{\text{both}} = m v_s \left[1 - \cos \alpha_1 \left(\cos^2 \alpha_1 - \frac{V^2}{v_s^2} \sin^2 \alpha_1 \right)^{1/2} - \sin \alpha_1 \left(\sin^2 \alpha_1 - \frac{V^2}{v_s^2} \cos^2 \alpha_1 \right)^{1/2} \right]. \quad (8)$$

If only one particle escapes, which occurs when $0 < \alpha_1 < \alpha_e$ or $\frac{\pi}{2} - \alpha_e < \alpha_1 < \frac{\pi}{2}$, the net momentum loss is (combining eqs. 5, 6, 7, 3, and 4):

$$p_{\text{one}} = m v_s \left[1 - \cos \alpha_1 \left(\cos^2 \alpha_1 - \frac{V^2}{v_s^2} \sin^2 \alpha_1 \right)^{1/2} \right]. \quad (9)$$

Now we should average the above momentum loss over all scattering angles. For this, it is convenient to use the reference frame of the center of mass of the colliding particles. In this frame, the scattering is isotropic, as long as the particles are "slow" in the sense that $m u r / \hbar \ll 1$, where r is the linear scale of the interaction and $u = v_0/2$ is the collision velocity (Landau & Lifshitz 1958, §132). For example, for rigid spheres with radius r (for which the scattering cross-section is $\sigma = 4\pi r^2$, Landau & Lifshitz 1958), the scattering is isotropic if

$$\left(\frac{m c^2}{1 \text{ GeV}} \right)^{3/2} \left(\frac{u}{2400 \text{ km s}^{-1}} \right) \left(\frac{\sigma/m}{50 \text{ cm}^2 \text{ g}^{-1}} \right)^{1/2} \ll 1 \quad (10)$$

Note that if the DM particles are WIMPs with the currently favored mass ($m c^2 > 40 \text{ GeV}$, Hagiwara et al. 2002), this condition is not satisfied for the values of $\sigma/m \sim (1-10) \text{ cm}^2 \text{ g}^{-1}$

that we are able to constrain. Scattering with such combinations of σ and m would be strongly beamed, reducing all the observable effects for a given σ . However, there is still ample parameter space for isotropic scattering (e.g., if particles are not WIMPs), and we will confine our estimates to this simple case. Our conclusions will be directly comparable to other astrophysical cross-section measurements which also implicitly assume isotropic scattering.

In this reference frame, particle 1 scatters by an angle $\theta = 2\alpha_1$ ($0 < \theta < \pi$) and particle 2 scatters by $\pi - \theta$. Combining eqs. (8, 9), weighting with solid angle and taking into account the symmetries, the average momentum lost by the subcluster in each particle collision is (for our values of V and v_s):

$$\bar{p} = mv_s \left[1 - 4 \int_{\sin \alpha_e}^1 x^2 \left\{ x^2 - \frac{V^2}{v_s^2} (1 - x^2) \right\}^{1/2} dx \right] \approx 0.1 mv_s. \quad (11)$$

When the subcluster with mass M_s (all in the form of dark matter for clarity) travels with a velocity v through the main cluster with density ρ_m , it experiences

$$n = \frac{M_s}{m} \frac{\sigma}{m} \rho_m v \quad (12)$$

collisions per second. As a result, it loses velocity, relative to the free-fall velocity v_{ff} :

$$\frac{d(v - v_{\text{ff}})}{dt} = \frac{\bar{p}n}{M_s} = \frac{\bar{p}}{m} \frac{\sigma}{m} \rho_m v, \quad (13)$$

where \bar{p} is from eq. (11). We conservatively disregard the higher subcluster velocity during core passage and assume that the loss of mass and velocity is relatively small, so \bar{p} is roughly constant. Integration of eq. (13) along the subcluster trajectory gives the total velocity loss. Noting that $\int \rho_m v dt = \int \rho_m dl$ is the mass column density of the main cluster along the subcluster's trajectory, Σ_m , we obtain

$$v - v_{\text{ff}} = \frac{\bar{p}}{m} \frac{\sigma}{m} \Sigma_m. \quad (14)$$

Almost all of Σ_m accumulates within the main cluster's core, at distances smaller than the current subcluster position. If, as we assume, the subcluster passed through the main cluster center, $\Sigma_m \simeq 0.3 \text{ g cm}^{-2}$; if it missed the center by 200–300 kpc, Σ_m is lower by about a factor of 2. On the other hand, we observe the main cluster after the collision; if it used to have an NFW-type peak disrupted by a direct hit of the subcluster, then Σ_m that we should use would be higher than the observed one.

Requiring that $v - v_{\text{ff}} < 1000 \text{ km s}^{-1}$, from eq. (14) we get

$$\frac{\sigma}{m} < 7 \text{ cm}^2 \text{ g}^{-1}. \quad (15)$$

2.3. The survival of the dark matter subcluster

For the observed subcluster mass and velocity, the most likely result of a particle collision is the loss of a particle by the subcluster. The opposite effect, i.e., accretion of the main cluster's particles, is negligible because of the low mass and high velocity of the subcluster. We can put an upper limit on the integrated mass loss and thereby on the collision cross-section. C04 have derived mass-to-light ratios for the subcluster within $r_{\text{tr}} = 150 \text{ kpc}$, $M/L_B \simeq 280 \pm 90$ and $M/L_I \simeq 170 \pm 50$. These ratios are in good agreement with the universal cluster values from the lensing analyses (e.g., Mellier 1999; Dahle 2000), and a factor of 1.1 ± 0.3 from the

main cluster values derived from the same data. If the subcluster had been continuously losing DM particles, we would expect an anomalously low M/L value for the subcluster — and in particular, a value lower than the main cluster's. From this agreement we can infer that the subcluster could not have lost more than $f \approx 0.2 - 0.3$ of its initial mass within r_{tr} . We should make two supporting comments here — first, the subcluster crossing time for its member galaxies is comparable to the time it took for the subcluster itself to cross the main cluster. Thus, if the subcluster's gravitational well has been slowly diminishing due to DM collisions, its galaxies did not have time to evaporate, so this process can be ignored. Second, although the main cluster's DM particles are similarly affected by the subcluster impact, the effect on the main cluster's M/L value is smaller by at least their mass ratio (about a factor of 6).

To escape beyond $r = r_{\text{tr}}$, the average subcluster particle needs a velocity $v_{\text{esc}} \simeq 1200 \text{ km s}^{-1}$. The subcluster experiences a net loss of a particle in a collision if both $v_1 > v_{\text{esc}}$ and $v_2 > v_{\text{esc}}$, which occurs at scattering angles θ given by (from eqs. 4):

$$\frac{v_{\text{esc}}}{v_0} < \sin \frac{\theta}{2} < \left(1 - \frac{v_{\text{esc}}^2}{v_0^2} \right)^{1/2}. \quad (16)$$

For our v_{esc} and v_0 , such angles exist. The probability of this loss, per collision, is

$$\chi = \frac{\int_{(16)} 2\pi \sin \theta d\theta}{\int_0^\pi 2\pi \sin \theta d\theta} = 1 - 2 \frac{v_{\text{esc}}^2}{v_0^2}, \quad (17)$$

where the upper integral is calculated over the interval of θ given by eq. (16). During the subcluster's transit through the main cluster, each of its original particles has a probability to collide

$$\tau_m = \frac{\sigma}{m} \Sigma_m. \quad (18)$$

Combining (17) and (18), the fraction of particles lost is

$$\chi \tau_m = \frac{\sigma}{m} \Sigma_m \left[1 - 2 \left(\frac{v'_{\text{esc}}}{v_0} \right)^2 \right], \quad (19)$$

where v'_{esc} is a slightly higher escape velocity that allows for the subcluster's mass decline by up to a factor of $1 + f$ along the way; $v'_{\text{esc}} \approx v_{\text{esc}}(1 + \sqrt{1 + f})/2$. We also ignore the subcluster's higher velocity at core passage, assuming the constant present velocity. (Both effects are small and our simplifications are conservative.) Requiring that $\chi \tau_m < f = 0.3$, from eq. (19) we obtain

$$\frac{\sigma}{m} < 1 \text{ cm}^2 \text{ g}^{-1}. \quad (20)$$

The expression in the brackets in eq. (19) is close to 1 for any small value of v_{esc} , thus our resulting constraint is only weakly dependent on the exact mass profile of the subcluster. We also note that the subcluster's M/L ratios derived by C04 represent lower bounds on the true values (because of possible projection and the particular technique employed to derive the subcluster mass), which makes our constraint conservative.

For cross-sections such as (20) and the subcluster's observed mass and radius, the mean scattering depth of the subcluster is $\tau_s \lesssim 0.2$. Thus our single-scattering assumption is reasonable as a first approximation. If one considers a possibility that the escaping particle may expel another subcluster particle, the probability (19) is a conservative underestimate. In §2.2, even higher τ_s are allowed by our resulting

limit (15); for that method, single scattering is also a conservative assumption. Inclusion of multiple scattering would lead to tighter limits, but requires detailed knowledge of the matter distribution inside the subcluster and is not warranted by the present data.

3. DISCUSSION

3.1. Improving the constraints

From the above order-of-magnitude estimates, the most promising way of improving the limit on (or measuring) the DM collision cross-section using 1E 0657–56 would be to refine the weak lensing mass map and limit (or detect) the mass loss from the subcluster core. Indeed, if it had lost a significant fraction of its DM particles, they should form a tail detectable in the dark matter map, not unlike the X-ray gas tail. This tail would, of course, be in addition to the matter tidally stripped from the subcluster and a gravitational wake discussed by Furlanetto & Loeb (2002). The main cluster’s DM particles also would be scattered, probably resulting in additional detectable effects in the mass map. These considerations, along with the conservative assumptions that we made throughout to simplify calculations, suggest that the best way to proceed with the data interpretation is a detailed hydrodynamic simulation of this merger, such as that performed by Tormen, Moscardini, & Yoshida (2003) but with the inclusion of collisionless galaxies and collisional DM with various cross-sections, followed by comparison of the results with the X-ray, optical and lensing data.

3.2. Astrophysical context

The nature of dark matter is still a great unsolved astrophysical problem. Laboratory searches for the DM candidates succeeded in showing that any interaction between the dark and baryonic matter is vanishingly small, with cross-sections many orders of magnitude lower than the values we consider in this work (e.g., Bernabei et al. 2003 and references therein). Despite their size, galaxy clusters have an average projected mass density of order $0.1 - 1 \text{ g cm}^{-2}$, so they are no match for the laboratory experiments for constraining the DM-baryon interactions. However, clusters and galaxies may provide the best available laboratory for studying the DM self-interaction.

While the common wisdom holds that DM is collisionless, a hypothesis of self-interacting dark matter (SIDM) with cross-sections of order $1 - 100 \text{ cm}^2 \text{ g}^{-1}$ was most recently proposed by Spergel & Steinhardt (2000) to alleviate several apparent problems of the collisionless CDM model, such as the non-observation of predicted cuspy mass profiles in galaxies (e.g., Moore 1994; Flores & Primack 1994; cf. Navarro, Frenk, & White 1997; Moore et al. 1999b) and overprediction of small sub-halos within the larger systems (e.g., Klypin et al. 1999; Moore et al. 1999a). Simulations and theoretical studies (e.g., Davé et al. 2001; Ahn & Shapiro 2002) narrowed the range required to explain the galaxy profiles to $\sigma/m \sim 0.5 - 5 \text{ cm}^2 \text{ g}^{-1}$ and pointed out that fluid-like DM with $\sigma/m \sim 10^4 \text{ cm}^2 \text{ g}^{-1}$ is another possibility.

Several observational constraints have been reported. Gnedin & Ostriker (2001; see also Hennawi & Ostriker 2002) pointed out that unless $\sigma/m < 0.3 - 1 \text{ cm}^2 \text{ g}^{-1}$, galactic halos inside clusters should evaporate on the Hubble timescale, because of collisional heat conduction from the hot cluster DM particles into the cool halos. We note that our constraint in §2.3 uses a very similar idea, except that we have a cluster-sized halo subjected to a flow of particles from one direction instead of random bombardment.

Furlanetto & Loeb (2002) proposed to use the different shapes of a gravitational wake that a subcluster halo moving through a bigger halo would create in the collisionless and fluid-like DM models. They argue that the X-ray image of the bright galaxy in the Fornax cluster already disfavors fluid-like DM. Their method is somewhat similar to our 1E 0657–56 estimates in that it also uses the motion of a halo within a bigger halo, but appears more observationally challenging. Following another suggestion of Furlanetto & Loeb (2002), Nataraajan et al. (2002) used observed sizes of the galactic halos in the A2218 cluster (which should be truncated at different radii for different DM cross-sections) to obtain $\sigma/m < 40 \text{ cm}^2 \text{ g}^{-1}$. Upper limits in the $0.02 - 10 \text{ cm}^2 \text{ g}^{-1}$ range were derived by Hennawi & Ostriker (2002) from the absence of supermassive black holes in the centers of galaxies.

Strong constraints are reported from the galaxy cluster cores. Yoshida et al. (2000) simulated evolution of a cluster for $\sigma/m = 10, 1, \text{ and } 0.1 \text{ cm}^2 \text{ g}^{-1}$ and obtained systematically flatter radial mass profiles for higher σ/m . Using *Chandra* X-ray data and the assumption of hydrostatic equilibrium, Arabadjijs et al. (2002) derived a mass profile for the cluster MS 1358+62 that is strongly centrally peaked (in fact, more peaked than even the collisionless simulations predict). From the comparison with Yoshida et al. (2000), they conclude that $\sigma/m < 0.1 \text{ cm}^2 \text{ g}^{-1}$. There are two potential difficulties with this stringent limit, however. *Chandra* revealed widespread gas sloshing in the cores of “relaxed” clusters (Markevitch, Vikhlinin, & Forman 2002), including in MS 1358+62, which does not lend support to the hydrostatic equilibrium assumption and the resulting X-ray mass estimates at relevant radii. More importantly, Yoshida et al. present time evolution of their simulated cluster profile for $\sigma/m = 10 \text{ cm}^2 \text{ g}^{-1}$, which at different epochs covers a range of shapes comparable to the whole difference between their 0.1 and $10 \text{ cm}^2 \text{ g}^{-1}$ simulations (see also Hennawi & Ostriker 2002). This suggests that for a high σ/m , one expects a variety of cluster mass profiles — and indeed, while many real-world clusters exhibit peaked profiles, a large fraction has flat cores (e.g., Coma). Therefore, a sample of cluster profiles is required for such studies. Miralda-Escudé (2002) used lensing data for the cluster MS 2137–23 to show that its central mass distribution is elliptical, and concluded that $\sigma/m < 0.02 \text{ cm}^2 \text{ g}^{-1}$, since otherwise DM collisions would erase ellipticity. Again, this interpretation may not be unique, because ellipticity may be affected by line-of-sight projections. This ambiguity is illustrated by the fact that Sand et al. (2002), using lensing data for the same cluster but considering the flatness of the central mass distribution instead of its ellipticity, arrived at the opposite conclusion.

While the above methods may eventually provide more sensitive constraints on σ/m than we have obtained, they require a statistical sample of clusters and cosmological simulations to reach solid conclusions. In comparison, the unique geometry of the 1E 0657–56 cluster merger allows us to see directly the (cumulative) results of single DM particle collisions, which makes the resulting limits quite robust.

Finally, we note that our limit, $\sigma/m < 1 \text{ cm}^2 \text{ g}^{-1}$, excludes most of the $0.5 - 5 \text{ cm}^2 \text{ g}^{-1}$ interval proposed to explain the flat mass profiles in galaxies. Within the SIDM paradigm, the galaxy profiles and the tight cross-section limits coming from clusters can still be reconciled if the cross-section were velocity-dependent, so that it would be smaller on average in clusters than in galaxies (e.g., Firmani et al. 2000, 2001;

Hennawi & Ostriker 2002; Colín et al. 2002). However, it is difficult to justify this additional degree of freedom in the model until a nonzero cross-section is detected at any velocity.

4. SUMMARY

We have combined new X-ray, optical and weak lensing observations of the unique merging cluster 1E 0657–56 to derive a simple, direct upper limit on the dark matter collisional cross-section, $\sigma/m < 1 \text{ cm}^2 \text{ g}^{-1}$. This is only an order-of-magnitude estimate; a more accurate, and quite possibly stronger, limit may be derived through hydrodynamic simula-

tions of this merging system.

We thank Neal Dalal and the anonymous referee for helpful comments. Support for this work was provided by NASA contract NAS8-39073, *Chandra* grant GO2-3165X, and the Smithsonian Institution. AHG was supported under award AST-0407485 by an NSF Astronomy and Astrophysics Postdoctoral Fellowship; DC received support from Deutsche Forschungsgemeinschaft under the project SCHN 342/3-1.

REFERENCES

- Ahn, K., & Shapiro, P. R. 2002, *J. Korean Astronomical Soc.*, 36, 89 (astro-ph/0212575)
- Arabadjis, J. S., Bautz, M. W., & Garmire, G. P. 2002, *ApJ*, 572, 66
- Barrena, R., Biviano, A., Ramella, M., Falco, E. E., & Seitz, S. 2002, *A&A*, 386, 816
- Bernabei, R., et al. 2003, preprint astro-ph-0307403
- Colín, P., Avila-Reese, V., Valenzuela, O., & Firmani, C. 2002, *ApJ*, 581, 777
- Clowe, D., Gonzalez, A. H., & Markevitch, M. 2004, *ApJ*, in press; astro-ph/0312273 (C04)
- Dahle, H. 2000, *Proc. The NOT in the 2000's*, Eds. N. Bergvall, L. O. Takalo, & V. Piirola (Univ. of Turku), 45
- Davé, R., Spergel, D. N., Steinhardt, P. J., & Wandelt, B. D. 2001, *ApJ*, 547, 574
- Firmani, C., D’Onghia, E., Avila-Reese, V., Chincarini, G., & Hernández, X. 2000, *MNRAS*, 315, L29
- Firmani, C., D’Onghia, E., Chincarini, G., Hernández, X., & Avila-Reese, V. 2001, *MNRAS*, 321, 713
- Flores, R. A., & Primack, J. R. 1994, *ApJ*, 427, L1
- Furlanetto, S. R., & Loeb, A. 2002, *ApJ*, 565, 854
- Gnedin, O. Y., & Ostriker, J. P. 2001, *ApJ*, 561, 61
- Govoni, F., Markevitch, M., Vikhlinin, A., VanSpeybroeck, L., Feretti, L., & Giovannini, G. 2004, *ApJ*, in press (astro-ph/0401421)
- Hagiwara, K., et al. 2002, *Phys. Rev. D*, 66, 10001
- Hennawi, J. F., & Ostriker, J. P. 2002, *ApJ*, 572, 41
- Klypin, A., Kravtsov, A. V., Valenzuela, O., & Prada, F. 1999, *ApJ*, 522, 82
- Landau, L. D., & Lifshitz, E. M. 1958, *Quantum mechanics: non-relativistic theory* (London: Pergamon)
- Liang, H., Hunstead, R. W., Birkinshaw, M., & Andreani, P. 2000, *ApJ*, 544, 686
- Markevitch, M., Gonzalez, A. H., David, L., Vikhlinin, A., Murray, S., Forman, W., Jones, C., & Tucker, W. 2002, *ApJ*, 567, L27 (M02)
- Markevitch, M., Vikhlinin, A., & Forman, W. 2002, astro-ph/0208208
- Markevitch, M., et al. 2004, in preparation (M04)
- Mellier, Y. 1999, *ARA&A*, 37, 127
- Milgrom, M. 1983, *ApJ*, 270, 365
- Miralda-Escudé, J. 2002, *ApJ*, 564, 60
- Moore, B. 1994, *Nature*, 370, 629
- Moore, B., Ghigna, S., Governato, F., Lake, G., Quinn, T., Stadel, J., & Tozzi, P. 1999a, *ApJ*, 524, L19
- Moore, B., Quinn, T., Governato, F., Stadel, J., & Lake, G. 1999b, *MNRAS*, 310, 1147
- Natarajan, P., Loeb, A., Kneib, J., & Smail, I. 2002, *ApJ*, 580, L17
- Navarro, J. F., Frenk, C. S., & White, S. D. M. 1997, *ApJ*, 490, 493
- Sand, D. J., Treu, T., & Ellis, R. S. 2002, *ApJ*, 574, L129
- Spergel, D. N., & Steinhardt, P. J. 2000, *Phys. Rev. Lett.*, 84, 3760
- Tormen, G., Moscardini, L., & Yoshida, N. 2003, *MNRAS*, submitted (astro-ph/0304375)
- Tucker, W. H., Tananbaum, H., & Remillard, R. A. 1995, *ApJ*, 444, 532
- Yoshida, N., Springel, V., White, S. D. M., & Tormen, G. 2000, *ApJ*, 544, L87